



**HAL**  
open science

# Assessing new sensor-based volume measurement methods for high-throughput bulk density estimation in the field under various soil conditions

Guillaume Coulouma, Denis Feurer, Fabrice Vinatier, Olivier Huttel

## ► To cite this version:

Guillaume Coulouma, Denis Feurer, Fabrice Vinatier, Olivier Huttel. Assessing new sensor-based volume measurement methods for high-throughput bulk density estimation in the field under various soil conditions. *European Journal of Soil Science*, 2021, 10.1111/ejss.13115 . hal-03212399

**HAL Id: hal-03212399**

**<https://hal.inrae.fr/hal-03212399>**

Submitted on 3 Jan 2022

**HAL** is a multi-disciplinary open access archive for the deposit and dissemination of scientific research documents, whether they are published or not. The documents may come from teaching and research institutions in France or abroad, or from public or private research centers.

L'archive ouverte pluridisciplinaire **HAL**, est destinée au dépôt et à la diffusion de documents scientifiques de niveau recherche, publiés ou non, émanant des établissements d'enseignement et de recherche français ou étrangers, des laboratoires publics ou privés.



Distributed under a Creative Commons Attribution - NonCommercial 4.0 International License

**bulk density estimation in the field under various soil conditions**

Running title : new bulk density estimation in the field

COULOUMA\*, G., FEURER, D., VINATIER, F., HUTTEL, O.

*LISAH, Univ Montpellier, INRAE, IRD, Institut Agro, F-34060 Montpellier, France*

\*Corresponding Author : COULOUMA, G., Guillaume.coulouma@inrae.fr

**Abstract**

Soil bulk density (BD) is a key soil property in soil science. BD is measured at the scale of the soil horizon with conventional methods : core sampling and rubber balloon. Regardless of the method, BD measurement in the field is cumbersome and time-consuming, especially in stony soils, and new, less invasive methods have emerged but their measurement quality needs to be compared with conventional ones. The photogrammetric technique (SfM) consists of the reconstruction of a given scene in 3D from multi-view photographs. The aim of the present work is to assess the SfM as a rapid, accurate method of measuring the volume of undisturbed soil for BD measurements, regardless of the soil depth and stone content. Ten soil horizons were investigated from various types of soils with different soil properties, especially texture (10 to 48% of clay) and stone content (0 to 73%). The bulk density of each horizon was measured with a reference method (core sampling), an excavation method (rubber balloon) and two recently developed sensor-based methods: SfM and a lightweight flash lidar. For the sensor-based methods, an automated post-processing method was developed to reduce the human operating time. The BDs measured from the SfM were significantly similar to those measured from core sampling. At this stage, the lightweight flash lidar is not sufficient to measure the BD with high accuracy. Finally, we recommend the use of SfM to measure BD regarding its robustness in varying soil conditions, especially stony soils and we discussed the potential of the method regarding the recent advances on its field use with smartphones.

**1. Introduction**

Soil bulk density (BD) is a key soil property in soil science. BD is related to soil porosity, which strongly influences the calculation of carbon content (Goidts et al., 2009), soil available water capacity and nutrient estimation in the soil. Al Shamary et al. (2018) classify BD

This article has been accepted for publication and undergone full peer review but has not been through the copyediting, typesetting, pagination and proofreading process which may lead to differences between this version and the Version of Record. Please cite this article as doi: 10.1002/ejss.13115

measurement methods as direct or indirect measurements. The core, excavation and clod methods involve direct measurements of the undisturbed volume of soil samples in the field (core and excavation) or in the laboratory (clod or excavation). Radiation methods such as gamma rays (for example, Bertuzzi et al., 1987) rely on indirect measurements in the field and require time-consuming calibration as well as precautions related to the radiation. Whatever the available method, the measurement of BD is time-consuming and generally requires soil pits to be dug to allow accurate BD measurements. Consequently, BD data are sparse in existing soil databases, which prevent the use of these databases as, for example, inputs for carbon stock calculations (Walter et al., 2016). Pedotransfer functions are commonly used for the prediction of BD (Qiao et al., 2019; Chen et al., 2018) based on relationships between well-characterized soil variables (for example, texture and organic carbon content) and bulk density measurements.

The effectiveness of conventional methods used to measure BD at the scale of the soil horizon, such as core sampling and rubber balloon, are also limited by its stone content. The core method is currently considered the standard method for direct BD estimation (Blake and Hartge, 1986). However, the reference core volume varies across studies and results in biases in the measured BDs (Terry et al. 1981). Terry et al. (1981) found that smaller cores ( $33 \text{ cm}^3$ ) enhanced the compression effect and that larger cores ( $2792 \text{ cm}^3$ ) captured macroporosity in the case of forest soils without gravel or stones. Moreover, the core sampling method is not applicable everywhere. The core sampling method is not usable in the case of stony soils or soils without sufficient structure. Excavation methods are then an alternative. The principle of the excavation method is based on the direct measurement in the field of the undisturbed volume with water, sand or Styrofoam balls (Grossman and Reinsch, 2002). To prevent the loss of water due to infiltration, different imaginative ways to seal the border of the excavation have been developed. The rubber balloon method replaces the void spaces with a rubber balloon filled with a volume of water directly measured on the excavation tool (Andraski et al. 1991). In the same way, Van Remortel (1993) sealed the border of the excavation with plastic wrap. Excavation with foam (Laundre, 1989) or plaster (Frisbie et al., 2014; Scanlan et al., 2018) is also a satisfactory method but is even more time-consuming than the other methods. Moreover, all of the excavation methods recommended in the case of stony soils are difficult to apply vertically (Brye et al., 2004). Finally, the clod method consists of sampling clods within the soil horizons and measuring their volume in the laboratory following different methods (Archimedes' principle, X-ray tomography, photogrammetry). The difficulties arise with disaggregation during transport and the risk of selecting specific hard soil structure features within the soil horizon. All of these methods have

been compared in the literature in terms of their effectiveness and cost as well as the representativeness of the measured BD (for example Al Shammary et al., 2018).

New developments have been made in the use of photogrammetry in terms of the number of available platforms, sensors, and software packages (Smith et al 2015). The structure from motion photogrammetric technique, denoted SfM hereafter, consists of the reconstruction of a given scene in 3D from multi-view photographs. Moret-Fernandez et al. (2016), and more recently Whiting et al. (2020) characterised the volume of small soil aggregates in the laboratory with SfM techniques. Bauer et al. (2014) tested SfM directly in the field on eight different soil surfaces and compared it with classical sand excavation for stony soils (4 out of 8 sites) and core methods for the rest. The SfM estimated the volume with a better precision than the sand replacement method. The comparison with the core method showed differences, mainly due to soil surface cracks that were not sampled in the cores. In the same way, 3D scanning methods were applied to BD measurement in the laboratory by Rossi et al. (2008) with a laser scanner on soil aggregates and most recently, Bagnall et al (2020) characterised the soil structure from the pit flank with a lidar. Scanlan et al. (2018) also used a Kinect sensor from the soil surface but with depth increments to characterize the BD at four different depths within the same excavation. The authors compared the volume calculated from the scanning system with the volume from a classical plaster cast of the excavation hole. The differences were exacerbated in the deeper measurements due to border effects. More recently, Polyakov et al. (2019) proposed terrestrial LiDAR as an alternative to the classical excavation method in stony soils for BD measurements at the surface with strong limitations due to the technical requirements and the cost of the device.

However, these promising techniques were only tested in horizontal situations and from the soil surface (Bauer et al., 2014; Scanlan et al., 2018; Polyakov et al., 2019). For example, Brye et al. (2004) already note the need to measure BD along the exposed face of soil profiles, especially in the case of stony soils. The punctual soil investigations require a vertical approach through the horizonation within the soil pits to obtain a large set of soil property measurements (Hartemink and Minasny, 2014). Currently, there is a lack of study on the comparison of conventional versus new sensor based methods in situ for a large range of soils.

Considering the need for BD data in many soil science applications, the aim of the present work is to assess SfM as an all-terrain method capable of overcoming the limitations of conventional methods for BD measurements, regardless of the stone content. Moreover, a simple and inexpensive 3D sensor is simultaneously tested with photogrammetry and other classical methods used as references: core sampling and the rubber balloon method. To the best of our

knowledge, our study is the first to assess and compare these four techniques on the same horizons with investigations both from above and from the side of the pit. Starting with a brief description of all the methods tested in the study, their associated protocols and their corresponding operating times, we compared all combinations of methods on the basis of a complete field dataset covering a large range of stone contents, organic carbon, textures, and structures.

## 2. Material and methods

### 2.1. Study area

The seven investigated pits that constitute the experimental dataset of this study were located in five study areas, all included in the Languedoc (southern France). They were selected to be representative of the diversity of soil characteristics that may change the bulk density measurement conditions (e.g., coarse fragments, texture, soil depth) and the bulk density itself (e.g., structure). A morphological description was performed on each pit according to the FAO guidelines for soil description (FAO, 2006). The final ten investigated horizons were chosen among this available different soil horizons, which is why not all the horizons at the same site were investigated. Five soil pits were dug in January, July and October 2018 for the Pech Rouge (43°08'33", 3°07'59"), Lavalette (43°08'33", 3°07'59") and Mauguio (43°35'33", 4°00'39") sites, respectively and two additional soil pits were investigated in September 2020 for the Angles (43°31'14", 2°31'45") and Restinclières (43°45'58", 3°51'15") sites. Samples of over 500 g were taken from each horizon for further laboratory characterization. The particle size distribution (texture), gravel and stone content, organic carbon content (OC), and calcium carbonate content (CaCO<sub>3</sub>) were measured at the French INRAE-ARRAS laboratory. Each sampled horizon is denoted (Site name)\_(Pit number when there were multiple pits in a site)\_H(horizon number, from top to bottom). Tables 1 and 2 summarize the characteristics of this soil dataset. Lavalette\_H2, Mauguio\_2\_H2, and Pech\_H2 correspond to deeply tilled horizons with high structural variability. Lavalette\_H4 and Mauguio\_1\_H3 show medium to high porosity due to high microfaunal activity. The clay content is highly variable between the investigated horizons, from 10% for Pech\_H2 to 48% for Mauguio\_3\_H2. The organic carbon is generally low except in the Angles\_H1 covered by

Douglas trees. Finally, the coarse fragment varied between low content in Mauguio\_H1 to a maximum in Mauguio\_3\_H2.

<Table 1 and 2 here>

## 2.2. Soil bulk density estimation

### 2.2.1 General experimental setup

Each of the ten horizons was investigated both on the side of the pit (core sampling, SfM, flash LiDAR) and from above after digging to reach the given horizon (rubber balloon, SfM, flash LiDAR).

<figure 1 here>

#### *Investigations from the vertical side of the horizons: core sampling, SfM and Flash LiDAR*

The first investigations were performed directly in the side of the pit (figure 1a) with the same procedure repeated for each investigated soil horizon. One unique flash lidar data acquisition of the whole horizon was performed immediately followed by an SfM acquisition that also covered the whole horizon. Both of these procedures were done *before* soil sampling. Then, five excavations were performed for each sampled horizon. Once the soil was sampled at these five locations, a second flash lidar acquisition of the whole soil horizon and a SfM acquisition of the whole horizon were performed *after* the soil sampling. Finally, three repetitions of core sampling with 100 cm<sup>3</sup> cores (Blacke and Hartge, 1986) were performed within each of the five excavations. Hence, the flash lidar data and SfM acquisitions imaged exactly the same volumes, while the core sampling method investigated its own fixed volume samples at the back of each excavation.

#### *Investigations from the horizontal side of the horizons: rubber balloon, SfM and Flash LiDAR*

For each investigated horizon, the same procedure described hereafter was used (figure 1b). First, soil was removed to constitute a planar horizontal surface at the average level of the five excavations previously dug from the sides of the pit in order to investigate the same zone (previous section) of a given soil horizon. Five excavations were performed, following the recommendation of the rubber balloon method (NF X31-502). For each excavation, exactly the same excavated volume was measured with three methods: rubber balloon, flash lidar and SfM. The same procedure was used as above, but with the addition of a density plate around each

excavation, fixed with iron fastening clips, which was necessitated by the rubber balloon acquisition (figure 1b). Adding a density plate to the protocol necessitated moving both the density plate and flash lidar from one excavation to another, leading to five acquisitions with each method for a given horizon, compared to only one acquisition from the side of the pit.

The following table (Table 3) summarizes the soil samples taken for each of the ten investigated horizons of the seven different pits.

<Table 3 here>

### 2.2.2 Laboratory sample processing for raw and fine bulk density estimation

The excavated samples were dried (48 h at 105°C) and weighed in the lab. Bulk densities ( $\rho_b$ ) were determined as the ratio between the dry soil mass and the total sampled volume. As some samples contained high volumes of gravels and stones, we calculated a fine earth bulk density ( $\rho_{bFE}$ ) without coarse fragments. To that end, each sample was sieved to extract the coarse fragments (e.g., >2 mm). There were different types of coarse fragments, and their density was measured following the classical method based on the Archimede's principle. The values varied between 1.9 for the highly weathered pebbles in Angles\_H1 to 2.6 for the limestones in Restinclières\_H1. The  $\rho_{bFE}$  was determined as the ratio between the dry soil mass without the coarse fragments and the total sampling volume without the volume corresponding to the coarse fragments. This latter volume was calculated from the mean bulk density of the coarse fragments given in table 2. Due to the large range of coarse fragments within the dataset, the  $\rho_{bFE}$  values were chosen to compare the methods.

## 2.3 Sensor-based volume measurement - data acquisition

For all the investigations, a canopy was used to obtain homogeneous lighting. The canopy was used to prevent shadowing and shade changes during sensor-based data acquisition and soil sampling.

### 2.3.1. Flash lidar

We used a PmdTec Pico Flexx flash lidar sensor operated from a smartphone and fixed on an angle iron so that it did not move between the *before* and *after* acquisitions. The sensor provides 224 x 171 3D frames with a given precision of 1% of the distance, which corresponds to the order of magnitude of the centimetre in our case (acquisition at approx. one metre).

Acquisition was performed over five seconds for median temporal filtering of the point cloud to decrease noise and eliminate outliers. For a minority of acquisitions, a small offset between the two point clouds was observed, most likely because the angle iron may have shifted during soil sampling. These particular point clouds were thus co-registered by using the ICP algorithm of CloudCompare 2.10.1.

### 2.3.2. SfM

We used a Nikon D3200 camera with an 18-55 mm AF Nikkor objective set at 18 mm with camera focus fixed so that camera parameters could be considered constant during the acquisitions. A convergent set of at least 20 images - both *before* and *after* soil sampling - was acquired to cover the whole area with multi-view stereoscopic imagery, including the scale bars with coded targets.

In the office, all images taken *before* and *after* excavation were processed with the Time-SIFT method (Feurer and Vinatier, 2018) using Agisoft Photoscan 1.2.6 to produce two 3D point clouds with the exact same geometric reference. Coded targets were used to scale the model. For soil samples taken from the side of the pit, a single pair of *before* and *after* point clouds was obtained for the whole horizon. For soil samples taken from above, there was one pair of *before* and *after* point clouds for each excavation.

## 2.4 Sensor-based data post-processing

### 2.4.1 Manual post-processing method

For the manual estimation of excavation volumes, 3D point clouds derived from flash lidar and/or SfM acquisition were processed together in the CloudCompare 2.10.1 software. A cloud-to-cloud distance was computed, and the 3D point clouds were coloured with this distance information. Each excavation was then manually delineated and clipped. Finally, the excavated volume was computed as a 2.5D volume on a 1 mm resolution grid.

### 2.4.2 Automatic post-processing method

After automatically trimming the borders of the excavations, dense 3D point clouds resulting from the flash lidar and SfM acquisitions were processed in several steps consisting of a combination of calls to CloudCompare 2.10.1 functions using R software and raster processes using the 'raster' R library. Excavated holes were detected using cloud-to-cloud distances between 3D point cloud before and after excavation, considering the minimal areas of the holes and the level of noises of the methods (Figure 2). The complete method is available as an R code in the open access repository Zenodo at the following URL (<https://doi.org/10.5281/zenodo.4036423>), and a sample dataset is available at the following URL (<https://doi.org/10.5281/zenodo.4036313>).

<Figure 2 here>

### 2.5. Comparison of operating times

The long operating time of core sampling is mainly due to the high number of samples required to improve the statistical significance of the measured bulk density. The other methods require similar, lower operating times. However, the rubber balloon method in the field is also time-consuming compared to the sensor-based methods (Table 4).

<Table 4 here>

### 2.6. Statistical analyses

First, manual and automatic processing for volume estimation were compared two-by-two (SfM and flash Lidar) using a linear model. Second, taking the automatic volume processing as the basis for volume calculations, volumes issued from SfM method were compared to those issued from rubber balloon and flash lidar using a linear model and the classical figures of merit ( $R^2$ , RMSE, intercept and slope) of the model as descriptors of the accuracy of the correlation between variables. Finally, all densities calculated from the automatic volume processing were compared using ANOVA considering the methods, horizons and replicates as explanatory variables. Reliability of the SfM method to the others was tested using differences in means and Tukey's HSD post hoc criterion.

### 3. Results

#### 3.1 Representativity of the dataset in terms of volumes and densities

##### 3.1.1 Range of raw density $\rho_b$

Based on the classical core sampling reference method, the studied horizons corresponded to a large observed range of  $\rho_b$  [1.04 - 1.71] mainly due to their various structural arrangements, organic carbon content and porosities. This dataset covered a large part of the bulk density measured in national databases (for example Hollis et al., 2012). The highest  $\rho_b$  values measured with core sampling were in Mauguio\_1\_H2, due to tillage and wheeling degradations. The highest  $\rho_b$  values (a mean of 2.01, measured in Mauguio\_3\_H2 with flash lidar and SfM) could not be measured with core sampling due to high pebble and gravel content (the highest : 73% in mass). The lower  $\rho_b$  values corresponded to the organic horizon Angles\_H1 (1.04). The  $\rho_{bFE}$  were lower than the  $\rho_b$  values due to the high content of coarse fragments in some horizons.

##### 3.1.2 Range of measured volumes

The distribution of the volumes measured with rubber balloon, SfM and flash lidar demonstrate a large range from 100 to 1400 cm<sup>3</sup>. The high number of measurements around the median (385 cm<sup>3</sup>) corresponded to the rubber balloon excavations.

#### 3.2. Comparison of the volume estimation from SfM, flash lidar, and rubber balloon

The automatic post-processing method used to estimate the volume from sensor-based methods was compared to the manual post-processing method. The automatically estimated volumes from both SfM and flash lidar were extremely similar to those estimated by the manual approach ( $R^2=0.998$ , RMSE of 11 cm<sup>3</sup>). Therefore, automatic post-processing was used in the rest of the analysis.

In the case of the investigation of the horizons from above, the excavations were sized for the rubber balloon method, and exactly the same holes were scanned by the flash lidar and SfM. Hence, for these samples, exactly the same volumes from the three methods were measured and compared. The volumes measured by rubber balloon were systematically greater than the volumes measured by SfM (intercept of the linear model = 12 cm<sup>3</sup>,  $P<0.05$  Student's t-test) (Figure 3a). Conversely, no bias was observed between the volumes from flash lidar and SfM (Figure 3b). However, the relationship between the volumes was noisy, especially at larger volumes, with an RMSE of 36 cm<sup>3</sup>.

<Figure 3 here >

### 3.3 Determination of the bulk densities at the horizon scale

<Table 5 here>

A comparison between the methods was conducted on the basis of the  $\rho_{bFE}$  (figure 4 and table 5). The  $\rho_{bFE}$  values measured from sensor-based methods were similar regardless of the soil characteristics, except for Lavalette\_H2 (Tukey's HSD test,  $P < 0.01$ ). However, the standard deviation of the flash lidar data was systematically higher than those of SFM. The significant noisy measurement of the volume (an RMSE of  $36 \text{ cm}^3$ ) directly corresponds to a high standard deviation of the resulting BD (more than 0.05 for a volume of  $1000 \text{ cm}^3$ ). The comparison between classical methods and SFM showed differences in relation to the coarse fragments. For low content of coarse fragments (i.e.  $< 15\%$  in mass), The  $\rho_{bFE}$  values measured from core sampling were significantly the same of those from SFM (Tukey's HSD test,  $P < 0.01$ ), except for Manguio\_1\_H3 and Manguio\_2\_H2. Moreover, the standard deviations of  $\rho_{bFE}$  from both core sampling and SfM measured within each horizon were also similar. The  $\rho_{bFE}$  values measured from rubber balloon was systematically lower than that measured from SFM and significantly lower for Lavalette\_H2, Manguio\_3\_H3, and Pech\_2 (Tukey's HSD test,  $P < 0.01$ ).

figure 4 here>

Conversely for high content of coarse fragments, the  $\rho_{bFE}$  measured from core sampling were always lower than the other methods, regardless of the other soil properties (Tables 5 and 2). Finally, the variability of the measurements was high whatever the methods. The flash lidar resulted to the highest standard deviation measured in the Angles\_H1 horizon and Manguio\_3\_H2 horizon (the highest coarse fragment content).

## 4. Discussion

The ten horizons were investigated both on the side of the pit (core sampling, SfM, flash LiDAR) and from above (rubber balloon, SfM, flash LiDAR). This methodology provided an original dataset which opens the discussion on the applicability and efficiency of each method. To the best of our knowledge, this study is the first experimental comparison of four different methods for soil bulk density measurement in a wide range of soil types and horizon depths.

### 4.1 Accuracy of SfM for soil bulk density measurement

The acquisition of the excavated volume is key for soil bulk density measurements. Reference core sampling uses a fixed volume to extract the bulk soil. The other methods, except gamma rays, depend on an excavated volume of soil. Of the SfM, rubber balloon and flash lidar methods, SfM provided the greatest improvement over the core sampling method in terms of its measurements of bulk density. This result is mainly due to the high accuracy of the volume measurement, which had a very low standard deviation. In line with the results from Bauer et al. (2014) from the soil surface, our study, applied to soil horizons, helped to cover all components of pedological studies. In addition, the measure of the volume with the rubber balloon was systematically higher than that measured by the SfM, leading to lower resulting bulk densities. This was already observed in many studies (Ship and Matelski, 1965; Yoro and Godo, 1990; Andraski et al., 1991; Page-Dumroese et al., 1999). The main proposed reason is that the size of the excavation is larger than the volume sampled with core sampling, and allows to better taking into account the structural porosity. In our study, exactly the same excavated volume was estimated with the rubber balloon, flash lidar and SfM methods. Therefore, our findings suggest that the volumes of the excavations may be systematically overestimated when measured with the rubber balloon, probably due to the overestimation of the first volume corresponding to the void between the edge of the device and the soil surface. Moreover, the pressure of the rubber balloon probably flattens out the edge of the excavation. These hypotheses are also corroborated by the bulk densities measured with core sampling, which showed no bias when compared with the bulk densities measured by SfM both from above and from the side of the pit. Our results may hence indicate that, in addition to the already known source of bias linked to larger investigated volumes, the rubber balloon method may have inherent flaws in the volume estimation itself. Moreover, the volume measured with rubber balloons seems to be noisier than that measured by SfM within the same horizon, especially when the gravel and pebble contents increase. The

balloon may not truly match the edges of the excavations, although the shape follows smooth edges during the excavation. The coarse gravels and pebbles may modify the contact between the balloon and the excavation edge and result in an increase in noise.

Excavation methods are generally used in the literature when the gravel and stone content of the soil exceeds 10% by mass. The different horizons tested in our study show the satisfactory applicability of the SfM method in these cases. Indeed, the total amount of gravel and stone varied from 0 to 73% (in mass), and the SfM method was not impacted by the gravel content. Similarly, the rubber balloon method is not recommended in the case of sandy textures due to the collapse of the excavation (Andraski et al., 1991). In our study, the SfM method succeeded in the sandy Pech\_H2 horizon (79% of sand). However, it must be noted that the bulk density was slightly overestimated compared to that estimated by core sampling.

Kutilek and Nielsen (1994) discussed about the representative elementary volume (REV) in Hydrodynamic and calculated a REV minor than  $100 \text{ cm}^3$  for poor structured soils and larger for well-structured soils. The core sampling with a fixed investigated volume is limiting in order to characterise structured soils. The size of the excavation for SfM measurement may be adapted to each situation to take into account the different specific porosities (small cracks, structural vughs, pebble size). This point was already made by Bauer et al. (2014) in the case of small soil surface cracks that could not be characterized by classical core sampling. Scanlan et al. (2018) noted the value of sizing the excavation to characterize different representative volumes. For example in Mauguio\_1\_H3 with a high porosity combined to a very clear structure, the volume investigated with the core sampling were lower than those from SfM and flash lidar (more than  $1000 \text{ cm}^3$ ) and probably did not include the structural porosity. Consequently, the  $\rho_{\text{bFE}}$  values from core sampling were higher than from the other methods. Finally, an additional advantage of SfM is its applicability regardless of the orientation of the soil face, along the side of the pit or from above.

#### 4.2 Displaying SfM from the field to the lab

In addition to the demonstrated accuracy and precision of the volume estimation both from above and from the side of the pit, a great advantage of the proposed SfM method is the very low time needed in the field (Table 4), as already noted in previous studies (Bauer et al., 2014; Scanlan et al., 2018). Moreover, the volume is directly measured in the field and any undisturbed samples need to be returned to the laboratory for fine volume measurement, as proposed SfM methods from Moret-Fernandez et al. (2016) or from Whiting et al. (2020). Field work is often performed under time constraints. The representativity of the sampling with only 5 samples (a total of 1500

cm<sup>3</sup> on average) is at least comparable to that of the core sampling with an equivalent of 15 samples. However, the sampling must follow important recommendations mainly: (i) maintain a smooth shape of the excavation, (ii) be careful to maintain a good lighting of the image without potential moving objects, and (iii) prevent external soil particles from falling during the excavation.

Almost all image data processing is automated, with the exception of the application of the Time-SIFT method. Currently, operator intervention is still needed between the two main steps (image alignment and dense matching) of Time-SIFT processing to separate the so-called *before* and *after* datasets prior to the computing of the dense 3D point clouds. This was not a limiting factor in the case of this study, which suggested that this study had a manageable amount of samples (several dozens), but may become a true limitation for the normal operational use of SfM-based soil bulk density measurements. There is hence a strong interest in developing a Time-SIFT plugin for Photoscan so that the whole image processing process would be fully automated, from image dataset provision to individual volume estimations. This work is already ongoing but is out of the scope of this study. Other further work may assess the potential for the use of simple sensors such as those on smartphones for image acquisition and further 3D processing. Even if the lens and sensor quality of smartphones is lower than that of single-lens reflex digital cameras, the quality of the latest phone cameras and the availability of multi-lens smartphones may provide enough quality to allow for accurate and precise volume measurements. A test realised on one excavation (data not shown) results in an excellent agreement between camera-based and phone-based SfM.

#### 4.3 The promise of flash lidar

The soil bulk densities measured from the flash lidar data were generally significantly different from the values estimated with other methods. A prominent finding is the large standard deviation of flash lidar data compared to that from the SfM method. This calls into question the accuracy of the flash lidar method, which also depends on a large set of local environmental conditions, such as wind and scene illumination. Compared with that in our results, Scanlan et al. (2018) achieved better accuracy on BD measurements while using a Kinect™ sensor. The main factor explaining the difference between our findings and the findings of Scanlan et al. (2018) is most likely the sensor resolution. The Kinect sensor used by these authors is a 2 M pixel sensor (1920x1080), while the Pico Flexx used in our study is only a 38 k pixel sensor (224 x 171). With such a small number of pixels, and especially for the case of the investigation on the side of the

pit, sampling of the 3D surface may not be sufficient to correctly depict the geometries before and after excavation. On the other hand, Polyakov et al. (2019) used a professional-grade terrestrial laser scanner whose accuracy and precision specifications are totally different from the specifications of the lightweight flash lidar such as the ones used in the study of Scanlan et al. (2018) and in this study. However, their work confirms the interest in using laser-based sensors for volume measurements, and our three studies definitely demonstrate the strong potential of 3D sensors for soil studies. Considering the differences among the sensors used in our three studies, it is still hard to determine whether continuous flash lidar scanning (as proposed by Scanlan et al. (2018) is needed to obtain the required precision and accuracy or whether a single point of view with time averaging (as we propose in our study), but with a better sensor would be sufficient. Regardless, the main advantages of using such lightweight range imaging sensors are their easy handling without prior specific knowledge and the large frame (more than 2 m<sup>2</sup>) recorded during just a few seconds. These devices also connect directly to a simple smartphone and do not need a single-lens reflex camera, which is advised for the SfM. Finally, it is expected that better lightweight flash lidar devices will become available and would allow the use of this method to obtain the required accuracy and precision for the volume estimations.

#### 4.4 The bulk density of fine earth from the stony soils

The studied dataset showed large differences with the measurement of bulk density in relation to the coarse fragment contents. Core sampling was considered as a reference for the measurement of bulk density in numerous studies. In case of low coarse fragment contents (i.e. <15%), the sampling was possible with the core sampling and a simple correction is sufficient to study the bulk density of the fine earth. Restinclieres\_H2 and Angles\_H1, with respectively 24 and 36 % in mass of coarse fragment contents, presented lower bulk densities of the fine earth than expected with the core sampling method. During the sampling in the field, the fine gravels and gravels were easily included in the core stainless steel and did not significantly deflect the driving of the core. However, the stones modified the driving and the structure of the sample. The resulting sample consequently contained lower quantity of fine earth. Conversely, the excavation methods undisturbed the structure of the fine earth whatever the gravel and stone content. The comparison with the core sampling was biased and conducted to an underestimation of  $\rho_{bFE}$  with the core sampling. In case of very high stone content (Mauguio\_3\_H2), the core sampling was

even not applicable at all. The sensor-based excavation methods denoted low and noisy  $\rho_{bFE}$  values, which probably depend on the irregular voids between the stones.

Stony soils (i.e. soils with more than 30 % in mass of coarse fragments) represent a large part of the Mediterranean soils and more generally of the European countries (The soil map of Europe, 2014). New studies focusing on the relation between stony soils and water retention show the importance of stones and the relation between stones and fine earth (for example, Korboulewsky et al. (2020)). The structural arrangements within the fine earth in stony soils needs to be studied and the new proposed excavation methods may improve future datasets.

## 5. Conclusion

Although BD is a key property in soil science, the classical methods for measuring BD in the field are time-consuming and present some limitations, especially in stony soils. The aim of the present work was to assess SfM as an all-terrain method capable of overcoming the limitations of conventional methods for BD measurements, regardless of the stone content. The SfM method provides accurate measurements with significantly less time in the field than the traditional method, regardless of the soil conditions. Moreover, the representativeness of the measurement is larger than that of the reference core sampling and is adjustable according to the size of the different soil porosities. The volume of excavations measured from rubber balloons, which are often used in the case of stony soils, is significantly higher than the volume measured from the SfM. This result confirms the bias of the rubber balloon method, which is often discussed in the literature. At this stage, lightweight flash lidar is not sufficient to measure BD with high accuracy. However, the flash lidar method is very accessible, and technical advances may provide more accurate devices in the future. Finally, the authors recommend the use of SfM to measure BD.

## 6. Acknowledgements

This study was directly supported by the LISAH research team. The authors thank N. Saurin for his kind help at the Pech Rouge site, the DIASCOPE team and Y. Blanca for their appreciated help at the Mauguio site.

Conflict of interest: None

Data availability statement:

R code <https://doi.org/10.5281/zenodo.4036423>

## 7. References

- Al-Shammary, A.A.G., Kouzani, A.Z., Kaynak, A., Khoo, S.Y., Norton, M., & Gates, W. (2018). Soil Bulk Density estimation methods: A review. *Pedosphere*, 28(4), 581-596.
- Andraski, B.J. (1991). Balloon and core sampling for determining Bulk Density of alluvial desert soil. *Soil Science Society of America Journal*, 55, 1188-1190.
- Bagnall, D.K., Jones, E.J., Balke, S., Morgan, C.L.S., & McBratney, A.B. (2020). An *in situ* method for quantifying tillage effects on soil structure using multistriple laser triangulation. *Geoderma* 380, in press.
- Bauer, T., Strauss, P., & Murer, E. (2014). A photogrammetric method for calculating soil bulk density. *Journal of Plant Nutrition and Soil Science*, 177, 496-499.
- Bertuzzi, P., Bruckler, L., Gabilly, Y., & Gaudu, J.C. (1987). Calibration, field testing, and error analysis of a gamma-ray probe for in situ measurement of dry bulk density. *Soil Science*, 144(6), 425-436.
- Blake, G.R., Hartge, K.H., 1986. Bulk density. In: Klute, A., Ed., *Methods of Soil Analysis, Part 1—Physical and Mineralogical Methods*, 2nd Edition, Agronomy Monograph 9, American Society of Agronomy—Soil Science Society of America, Madison, 363-382.
- Brye, K.R., Morris, T.L., Miller, D.M., Formica, S.J., & Van Eps, M.A. (2004). Estimating Bulk Density in vertically exposed stoney alluvium using a modified excavation method. *Journal of Environmental Quality*, 33, 1937-1942.
- Chen, S., Richer-de-Forges, A.C., Saby, N.P.A., Martin, M.P., Walter, C., & Arrouays, D. (2018). Building a pedotransfer function for soil bulk density on regional dataset and testing its validity over a larger area. *Geoderma*, 312, 52-63.
- FAO, 2006. *Guidelines for soil description*. Fourth edition. FAO, Rome
- Feurer, D., & Vinatier, F. (2018). Joining multi-epoch archival aerial images in a single SfM block allows 3-D change detection with almost exclusively image information. *ISPRS Journal of Photogrammetry and Remote Sensing*, 146, 495-506.
- Frisbie, J.A., Graham, R.C., & Lee, B.D. (2014). A plaster cast method for determining soil Bulk Density. *Soil Science*, 179, 103-106.

- Goidts, E., van Wesemael, B., & Crucifix, M. (2009). Magnitude and sources of uncertainties in soil organic carbon (SOC) stock assessments at various scales. *European Journal of Soil Science*, 60(5), 723-739.
- Grossman, R.B., & Reinsch, T.G. (2002). Bulk Density and linear extensibility, In: Dane, J.J., & Topp, G.C., Ed., *Methods of Soil Analysis, Part 4—Physical Methods*, 5.4—Soil Science Society of America, Madison, 201-228.
- Hartemink, A.E., and Minasny, B. (2014). Towards digital soil morphometrics. *Geoderma*, 230-231, 305-317.
- Hollis, J.M., Hannam, J., Bellamy, P.H. (2012). Empirically-derived pedotransfert functions for predicting bulk density in European soils. *European Journal of Soil Science* (63), 96-109.
- Korboulewsky, N., Tetegan, A., Szmouelian, A., & Cousin, I. (2020). Plants use water in the pores of rock fragments during drought. *Plant and Soil*, 454(1-2), 37-45.
- Kutilec, M., and Nielsen, D.R. (1994). *Soil Hydrology*. CATENA VERLAG. Germany
- Laundre, J.W. (1989). Estimating Soil Bulk Density with expanding polyurethane foam. *Soil Science*, 147, 223-224.
- Moret-Fernandez, D., Latorre, B., Pena, C., Gonzalez-Cebollada, C., & Lopez, M.V. (2016). Applicability of the photogrammetry technique to determine the volume and the bulk density of small soil aggregates. *Soil Research*, 54(3), 354-359.
- Page-Dumroese, D.S., Jurgensen, M.F., Brown, R.E., & Mroz, G.D. (1999). Comparison of methods for determining bulk densities of rocky forest soils. *Soil Science Society of America Journal*, 63, 379-383.
- Polyakov, V., Nearing, M., Nichols, M. H., Cavanaugh, M. (2019). An improved excavation method for measuring bulk density of rocky soil using terrestrial LiDAR. *Journal of Soil and Water Conservation*, 74(3), 319-322.
- Qiao, J., Zhu, Y., Jia, X., Huang, L., & Shao, M. (2019). Development of pedotransfer functions for predicting the bulk density in the critical zone on the Loess Plateau, China. *Journal of Soils and Sediments*, 19, 366-372.
- Rossi, A.M., Hirmas, D.R., Graham, R.C., & Stenberg, P.D. (2008). Bulk Density determination by automated three-dimensional laser scanning. *Soil Science Society of America Journal*, 72, 1591-1593.
- Scanlan, C. A., Rahmani, H., Bowles, R., Bennamoun, M. (2018). Three-dimensional scanning for measurement of bulk density in gravelly soils. *Soil Use and Management*, 34(3), 380-387.

- Ship, R.F., & Matelski, R.P. (1965). Bulk Density and coarse-fragment determinations on some Pennsylvania soils. *Soil Science*, 99, 392-397.
- Smith, M. W., Carrivick, J. L., & Quincey, D. J. (2015). Structure from motion photogrammetry in physical geography. *Progress in Physical Geography*, 40(2), 247–275.
- Terry, T.A., Cassel, D.K., & Wollum, A.G. (1981). Effect of soil sample size and included root and wood on bulk density of forested soils. *Soil Science Society of America Journal*, 45, 135-138.
- The Soil Map of Europe (2014). European Commission — Joint Research Centre Institute for Environment and Sustainability. [http://eusoils.jrc.ec.europa.eu/projects/soil\\_atlas](http://eusoils.jrc.ec.europa.eu/projects/soil_atlas).
- Van Remortel, R.D., & Shields, D.A. (1993). Comparison of clod and core methods for determination of Bulk Density. *Communication in Soil Science and Plant Analysis*, 24, 2517-2528.
- Walter, K., Don, A., Tiemeyer, B., & Freibauer, A. (2016). Determining Soil Bulk Density for Carbon Stock calculations: A systematic method comparison. *Soil Science Society of America Journal*, 80, 579-591.
- Whiting, M., Salley, S.W., James, D.K., Karl, J.W., & Brungard, C.W. (2020). Rapid bulk density measurement using mobile device photogrammetry. *Soil Science Society of America Journal*, 84, 811-817.
- Yoro, G., & Godo, G. (1990). Les méthodes de mesure de la densité apparente. Analyse de la dispersion des résultats dans un horizon donné. *Cahiers ORSTOM*, 25(4),423-429.

Table 1: Morphological properties of the investigated soil horizons

Investigated soil horizon	WRB Soil type	minimum depth (m)	maximum depth (m)	Colour	Structure		porosity	
					Type*	Size (mm)	pore level	type
Lavalette_H2	Calcisol	0.18	0.45	2.5Y44	SB/MA	20	medium/low	vughs
Lavalette_H4		0.60	1.90	2.5Y54	SB	30	very high	channels
Mauguio_1_H2	Fluvisol	0.65	1.00	2.5Y43	PR/SB	100/30	medium	vughs
Mauguio_1_H3		1.00	1.40	2.5Y64	SB	30	high	vughs
Mauguio_3_H2	Rhodic luvisol	0.45	0.75	5YR56	AB	10	low	-
Mauguio_3_H3		0.75	1.20	5YR44	AB	40	medium	-
Mauguio_2_H2	Fluvisol	0.40	0.80	10YR54	SB/MA	30	low	-
Pech_H2	Sandy Cambisol	0.35	0.60	10YR44	SB	30	low	-
Angles_H1	Cambic Umbrisol	0	0.35	10YR22	GR	10	medium	vughs
Restincliere_H2	Calcisol	0.10	0.25	10YR54	SB	20	medium	channels

\*according to FAO Guidelines for soil description (2006) : SB:subangular blocky; AB:angular blocky; MA:massive; PR:prismatic; GR:granular.

Table 2: Main physico-chemical properties of the investigated soil horizons

Investigated horizon	soil	fine gravel (%mass)	gravel/stones (%mass)	density of the coarse fragments	A (%)	L (%)	S (%)	Organic carbon (g/kg)	Calcium carbonate (g/kg)
Lavalette_H2		0	2	2.5	24	47	29	6.2	579
Lavalette_H4		0	0	2.5	27	47	26	4.1	734
Mauguio_1_H2		1	2	2.5	26	42	32	6	355
Mauguio_1_H3		1	0	2.5	23	39	38	4.5	367
Mauguio_3_H2		11	62	2.3	48	27	25	3.5	0
Mauguio_3_H3		3	3	2.3	45	33	22	2.4	0
Mauguio_2_H2		2	3	2.5	19	32	49	3.7	348
Pech_H2		4	8	2.5	10	11	79	5	306
Angles_H1		14	22	1.9	12	24	64	41	0
Restincliere_H2		8	16	2.6	20	42	38	6.7	749

Table 3: Characteristics of the soil samples and associated volume estimation methods.

Soil sample origin	Detailed location	Soil sampling method	Volume estimation method				number of samples
			SfM	flash lidar	rubber balloon	core sampling	
dug from the side of the pit	soil horizon	free excavation	same volume investigated		-	-	5 for each horizon
	background of the free excavations above	core samples	-	-	-	fixed volume* (100 cm <sup>3</sup> )	3x5 for each horizon
dug from above	hole of the density plate	free excavation	same volume investigated			-	5 for each horizon

\*for Mauguio\_3\_H2, the pebble content was too important to allow the core sampling method to be used

Table 4: Average human operating time (in min) of each method for one horizon with sufficient replications

Method (number of samples)	Time (min)				
	Field work		Lab work (except oven time)		Total count
	Soil sampling	Volume estimation	Soil weighing	Automatic sensor- based data pre- processing	
Core sampling (15)	45	-	15	-	60
Rubber balloon (5)	25	35	5	-	65
SfM (5)	15*	6	5	15	41
Lidar (5)	15*	1	5	15	36

*\*This time is lower mainly due to the ease of vertical sampling. In the case of horizontal sampling (rubber balloon), the excavation is time-consuming.*

Table 5: Mean soil bulk densities of fine earth ( $\rho_{bFE}$ ) measured by the different methods within each investigated horizon

Horizons	Coarse fragments (% in mass)	Sensor-based methods		Classical methods	
		SfM	Flash lidar	Rubber balloon	Core sampling
Lavalette_H4	0	<b>1.30 ± 0.06 (10)*</b>	<b>1.28 ± 0.14 (10)*</b>	<b>1.22 ± 0.07 (5)*</b>	<b>1.33 ± 0.06 (15)*</b>
Mauguio_1_H3	1	<b>1.53 ± 0.04 (10)*</b>	<b>1.45 ± 0.10 (10)*</b>	<b>1.47 ± 0.05 (5)*</b>	1.59 ± 0.03 (15)
Lavalette_H2	2	<b>1.63 ± 0.04 (10)*</b>	1.57 ± 0.04 (10)	1.55 ± 0.04 (5)	<b>1.65 ± 0.04 (15)*</b>
Mauguio_1_H2	3	<b>1.67 ± 0.04 (10)*</b>	<b>1.62 ± 0.10 (8)*</b>	<b>1.65 ± 0.09 (5)*</b>	<b>1.70 ± 0.07 (4)*</b>
Mauguio_2_H2	5	<b>1.64 ± 0.03 (10)*</b>	<b>1.56 ± 0.09 (10)*</b>	<b>1.57 ± 0.11 (5)*</b>	1.69 ± 0.05 (15)
Mauguio_3_H3	6	<b>1.59 ± 0.03 (10)*</b>	<b>1.68 ± 0.18 (10)*</b>	1.51 ± 0.06 (5)	<b>1.58 ± 0.04 (15)*</b>
Pech_H2	12	<b>1.66 ± 0.05 (4)*</b>	<b>1.70 ± 0.03 (2)*</b>	1.46 ± 0.08 (5)	<b>1.61 ± 0.07 (15)*</b>
Restinclières_H2	24	<b>1.43 ± 0.09 (10)*</b>	<b>1.41 ± 0.13 (10)*</b>	<b>1.39 ± 0.13 (5)*</b>	1.28 ± 0.13 (15)
Mingles_H1	36	<b>1.03 ± 0.07 (10)*</b>	<b>1.14 ± 0.23 (10)*</b>	<b>0.93 ± 0.08 (5)*</b>	0.88 ± 0.05 (14)
Mauguio_3_H2	73	<b>1.45 ± 0.22 (8)*</b>	<b>1.99 ± 1.42 (8)*</b>	<b>1.12 ± 0.18 (4)*</b>	-

Mean ± standard deviation (number of samples)

Horizons were ranked by their coarse fragment content, from low (Lavalette\_H4) to high (Mauguio\_3\_H2).

Bold cells with \* represent significantly equal means for each line (Tukey's HSD based on the Student distribution, at  $P < 0.01$ ) comparing to SFM.

Scale bars  
for SfM

3 core samples  
in each excavation

Flash Lidar



Angle iron used to fasten  
the Flash Lidar mount

rubber balloon

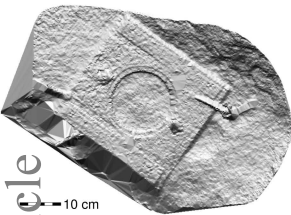
Density plate with  
scale bars for SfM

(a) - acquisition protocol and soil sampling in the flank of the pit

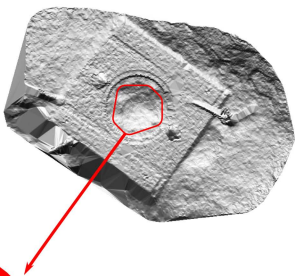
(b) - acquisition protocol from above

Accepted Article

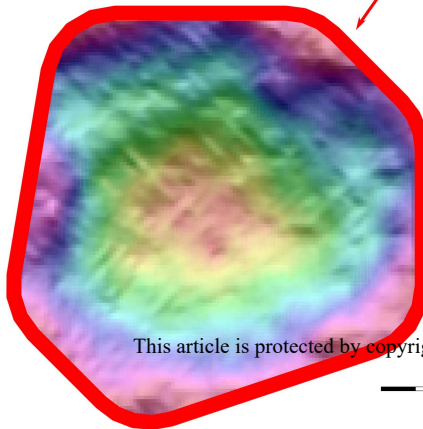
**Before excavation**



**After excavation**



Accepted Article



**cloud to cloud  
distance (in  $\mu\text{m}$ )**

0.00

-0.01

-0.02

-0.03

This article is protected by copyright. All rights reserved.

2 cm

